ГИАБ. Горный информационно-аналитический бюллетень /
MIAB. Mining Informational and Analytical Bulletin, 2024;(4):86-103
ОРИГИНАЛЬНАЯ СТАТЬЯ / ORIGINAL PAPER

УДК 550.8+550.4+550.3 DOI: 10.25018/0236_1493_2024_4_0_86

ГЕОХИМИЯ И ПЕТРОГРАФИЯ СКАРНОВОГО ОРУДЕНЕНИЯ, СВЯЗАННОГО С МАССИВОМ СЫРОСТАН, МИАССКИЙ РЕГИОН (ЮЖНЫЙ УРАЛ)

Ибрахим Мохаммед Абдалла Альшариф[1], А.Е. Котельников[1], А.Ф. Георгиевский[1], Ибрахим Самия Абдельрахман[2], Мусаб Хассан[1], Анас Мухаммад Абкар Баби[3]

[1] Департамент недропользования и нефтегазового дела, Инженерная академия, Российский университет дружбы народов, Москва, Россия, e-mail: mohammedelsharif7@gmail.com
[2] Департамент геологии, Факультет естественных наук, Хартумский университет, Судан
[3] Факультет нефтегазовой геологии и полезных ископаемых, Университет Бахри, Судан

Аннотация: В скарне обнаружено значительное количество металлов, в том числе W, Sn, Mo и Cu. Скарновая минерализация обнаружена в юго-западном направлении от города Миасса, в контакте диоритов и мраморов Сыростанского массива. Дано петрографическое и геохимическое описание скарновых пород. Для геохимического анализа с помощью ICP-MS, EMPA, рентгеноспектрального флуоресцентного анализа и петрографического исследования мы отобрали образцы как скарновых, так и магматических пород Сыростанского массива. Петрографическое исследование показало, что в минеральном составе скарна преобладают гранат, эпидот, амфибол и пироксен. Выделения граната и пироксена представлены ранней метасоматической стадией. Ретроградные изменения отличаются присутствием эпидота, кварца, кальцита и хлорита. Скарн связан с массивом Сыростан, в котором преобладают метаалюминиевые граниты I типа и гранитные породы кальциево-щелочной серии с высоким содержанием K. По сравнению с магматическими породами (гранитом и диоритом), образец скарна показал высокое обогащение HREE. Скарн, по-видимому, содержал более высокие концентрации Mo, W, Sn, Ta и Nb, чем породы, образующие массив. Содержащиеся в скранах оксиды железа, в которых соотношение Co/Ni (2,5–5,5), демонстрируют гидротермальное воздействие на магматический источник. Основываясь на этих результатах, мы предполагаем, что в скарне может происходить минерализация W, Sn и оксида железа.

Ключевые слова: геохимия, петрография, скарновая минерализация, ретроградные изменения, гидротермальный процесс, окись железа, Сыростанский массив.

Благодарность: Публикация выполнена при поддержке Программы стратегического академического лидерства РУДН.

Для цитирования: *Ибрахим Мохаммед Абдалла Альшариф, Котельников А. Е., Георгиевский А. Ф., Ибрахим Самия Абдельрахман, Мусаб Хассан, Анас Мухаммад Абкар Баби* Геохимия и петрография скарнового оруденения, связанного с массивом Сыростан, Миасский регион (Южный Урал) // Горный информационно-аналитический бюллетень. – 2024. – № 4. – С. 86–103. DOI: 10.25018/0236_1493_2024_4_0_86.

Geochemistry and petrography of skarn mineralization associated with Syrostan massive, Miass region (Southern Ural)

Mohammed Abdalla Elsharif Ibrahim[1], A.E. Kotelnikov[1], A.F. Georgievskiy[1], Samia Abdelrahman Ibrahim[2], Musab Hassan[1], Anas Mohamed Abaker Babai[3]

[1] Department of Mineral Development and Oil and Gas Engineering, Academy of Engineering, Peoples' Friendship University of Russia (RUDN University), Moscow, Russia, e-mail: mohammedelsharif7@gmail.com

[2] Department of Geology, Faculty of Natural Sciences, University of Khartoum, Sudan,

[3] Faculty of Petroleum Geology and Minerals, University of Bahri, Sudan

Abstract: A considerable type of deposits, including those for W, Sn, Mo, and Cu, are found in the skarn. Skarn mineralization can be found southwest of Miass City, near the boundary between marble deposits and diorite in massive complex. We describe the Skarn's petrography and geochemistry in this research. For our geochemical analysis with ICP-MS, EMPA, and X-ray spectral fluorescence analysis and petrography study, we collected samples of both the skarn and igneous rocks in the Syrostan massive. Petrography study revealed that garnet, epidote, amphibole, and pyroxene dominate skarn mineralization. Garnet and pyroxene minerals represent early metasomatic stage, indicating a prograde stage of alteration. Retrograde alteration, is distinguished by the presence of epidote, quartz, calcite, and chlorite. The skarn is associated with Syrostan massive, which dominant by metaluminous I-type granite and high-K calc-alkaline series granitic rocks. In comparison to igneous rocks granite and diorite, the skarn sample showed high enrichment in HREE. Skarn samples appeared to have higher concentrations of Mo, W, Sn, Ta, and Nb than igneous rocks form the Syrostan massive. skarn mineralization containing iron oxides, the Co/Ni ratios in the iron oxide (2.5 to 5.5) describe how the hydrothermal process affects the magmatic source. Based on these findings, we propose that W, Sn, and iron oxide mineralization may occur in skarn.

Key words: geochemistry, petrography, skarn mineralization, Retrograde alteration, hydrothermal process, iron oxide, Syrostan massive.

Acknowledgements: This paper has been supported by the RUDN University Strategic Academic Leadership Program.

For citation: Mohammed Abdalla Elsharif Ibrahim, Kotelnikov A. E., Georgievskiy A. F., Samia Abdelrahman Ibrahim, Musab Hassan, Anas Mohamed Abaker Babai Geochemistry and petrography of skarn mineralization associated with Syrostan massive, Miass region (Southern Ural). *MIAB. Mining Inf. Anal. Bull.* 2024;(4):86-103. DOI: 10.25018/0236_1493_2024_4_0_86.

Introduction

Skarn mineralization, characteristically formed by the contact of the carbonate-bearing host rocks and magmatic hydrothermal fluids. Globally, skarn deposits are the most essential source of significant metals and play a crucial role in sustainable development [1—4]. Field geology integrated with geochemical investigation is a significant key to mineral exploration for skarn mineralization [5—7]. The Southern Ural is well known as a resource for the large number of mineral deposits (e.g., Au, Cr, Cu, and REE) [8—11].

Deposits of tungsten, lithium, copper, molybdenum, etc., associated with magmatic intrusion, were revealed worldwide. Economic metals found in skarn deposits

include Fe, Cu, Sn, W, Pb, Zn, Ag, and Au [12–14].

Many studies [15–17] have found that skarn mineralization and deposits are widely distributed in the southern Ural. Additionally, Skarn alteration was recognized in the study area, the Southern Ural (Miass region) in the contact between diorite rocks belonging to Syrostan massive and the Marble Deposit of the Dark Kingdom [18].

Despite, the fact that the study area has been extensively investigated for gold mineralization [18], very little is known about skarn mineralization associated with magmatic intrusions [1, 2]. Furthermore, although numerous geochemical and geological studies of massive sulfide and gold deposits have been carried out [8, 9, 19, 20], the geochemistry and petrography of skarn alteration have been largely overlooked. The main objective of this research is to identify the geochemistry and petrography of skarn mineralization and reveal potential mineralization deposition of W, Sn, Mo, and REEs. These results provide primarily geochemical characteristics of skarn mineralization, mineralogy, and concentrations of possible deposition.

Samples and Analytical Methods

Field and geological observation

The field investigation was carried out during a field trip to the southern Ural, Miass region, by the Department of Mineral Development and Oil & Gas Engineering,

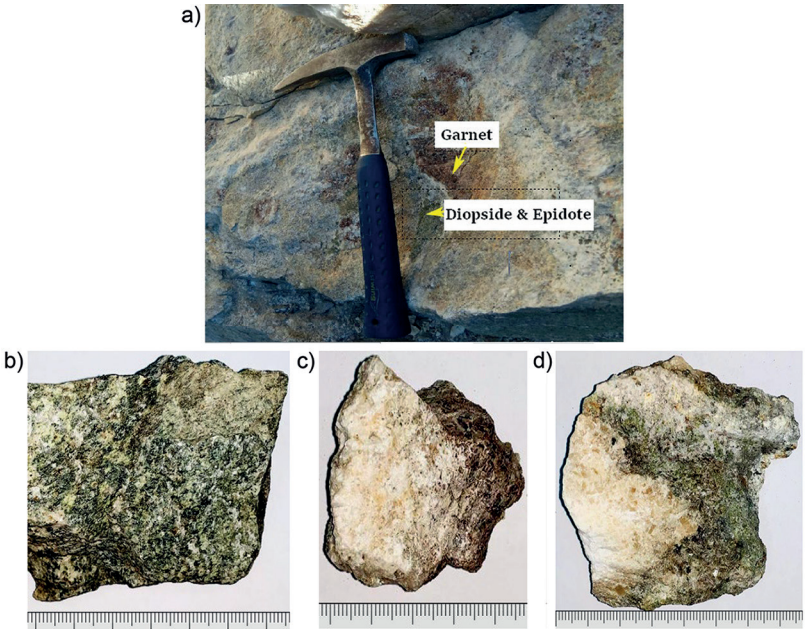

Fig. 1. Field images of skarn mineralization taken during the primary authors' research in the study area and published in their work [16]: clearly shows skarn alteration on the altered wall rock and the minerals associated with it (garnet, diopside and epidote) (a); contact between diorite and carbonate in which mineralization occur (b); skarn enrich with garnet mineral (c); carbonate-metasomatic alteration contact formed at the alteration wall of carbonate rocks (d)

Рис. 1. Изображения скарновой минерализации, полученные авторами ранее во время проведения полевых изысканий в районе исследования и опубликованные в работе [16]: измененный скарн в боковой породе и сопутствующие минералы (гранат, диопсид, эпидот) (а); минерализованный контакт диорита и карбоната (б); обогащенный гранатом скарн (в); контактная поверхность между карбонатными и метасоматическими породами в боковых измененных карбонатных породах (г)

People's Friendship University of Russia. Remarkably, Skarn alteration was observed in the contact between the Marble Deposit (Dark Kingdom) and the diorite (Syrostan massive).

Samples were taken from the altered wall rock (Skarnification) at the interface of carbonate and granitoid intrusions (Fig. 1, *a–d*). In addition to the primary marble body, the metamorphogenic complex is made up of the marble's countless small shards that are dispersed throughout diorite rock and encased in the form of xenoliths. The border between marbles and diorites is of a mixed kind; in certain locations, it is twisting with obvious traces of marble injection absorption by entering diorite magma. In other instances, the boundary is smooth and straight and coincides with slip joints, indicating the border is tectonic in origin. The dike-vein complex is geographically closely related to the diorites and the marble xenoliths that are found within them. The diorite complex and marble xenoliths are partially penetrated by microgranite veins that run along weaker zones at the diorite and marble boundary.

They grow into narrow rims ranging in size from millimeters to centimeters. In some cases, skarns form in tectonically disturbed marbles as nests and pockets with diameters ranging from 1 to 2 m. These are ribbon-shaped straight or bending entities that are observed in marble xenoliths and at their contacts with diorites.

Field investigation indicates that the skarn alteration is dominated by epidote, garnet, and pyroxene, suggesting an exoskarn edge. Besides skarn alteration, samples representing intrusion rocks have been collected.

Analytical methods

After intensive petrographic investigation, rock samples of granitoids and two samples of skarn was analyzed for bulk-rock major geochemical composition. Using a sequential vacuum spectrometer (with wavelength dispersion), model Axios mAX made by PAN Analytical (Netherlands), X-ray spectral fluorescence analysis (XRF) was used to measure the content of petrogenic oxides and a few trace elements in the samples. Principal component analysis was performed using the NSAM VIMS 439-RS method. To study the chemical composition using this technique, glassy discs were made from the sample material by induction melting of samples with lithium borates at a temperature of 1150 degrees C., which were analyzed in the spectrometer. Determination of weight loss on ignition is performed at a temperature of 1000 degrees C. according to the NSAM methodology SIMS 118-X. The analysis was performed at the Center for Collective Use of the IGEM RAS (Moscow, Russia).

Trace, rare and rare earth elements (REE) contents in rock samples, from intrusions and one representative sample of skarn mineralization were measured by inductively coupled plasma mass spectrometry (ICP-MS) for the sample at «IMGRE» lab (Russia). This experiment was applied for the detection and quantification of rare earth elements (REE) and trace elements, using the Agilent Series 7500. Approximately 0.05 g of sample powder was dissolved in solutions of HF + $HClO_4$ and then HF doped HNO_3 + HCl through a series of heating and evaporation stages to produce the sample. The solution was diluted by a factor of 50,000 after full dissolution.

JXA 8100 electron probe microanalysis system to determine the mineralogical characteristic of the skarn mineralization was used. The EMPA were performed at VIMS, Moscow, Russia, rock forming minerals of skarn were determined. The parameters were 20 kv, beam current $2 \cdot 10^{-8}$ A, and beam size 21 μm.

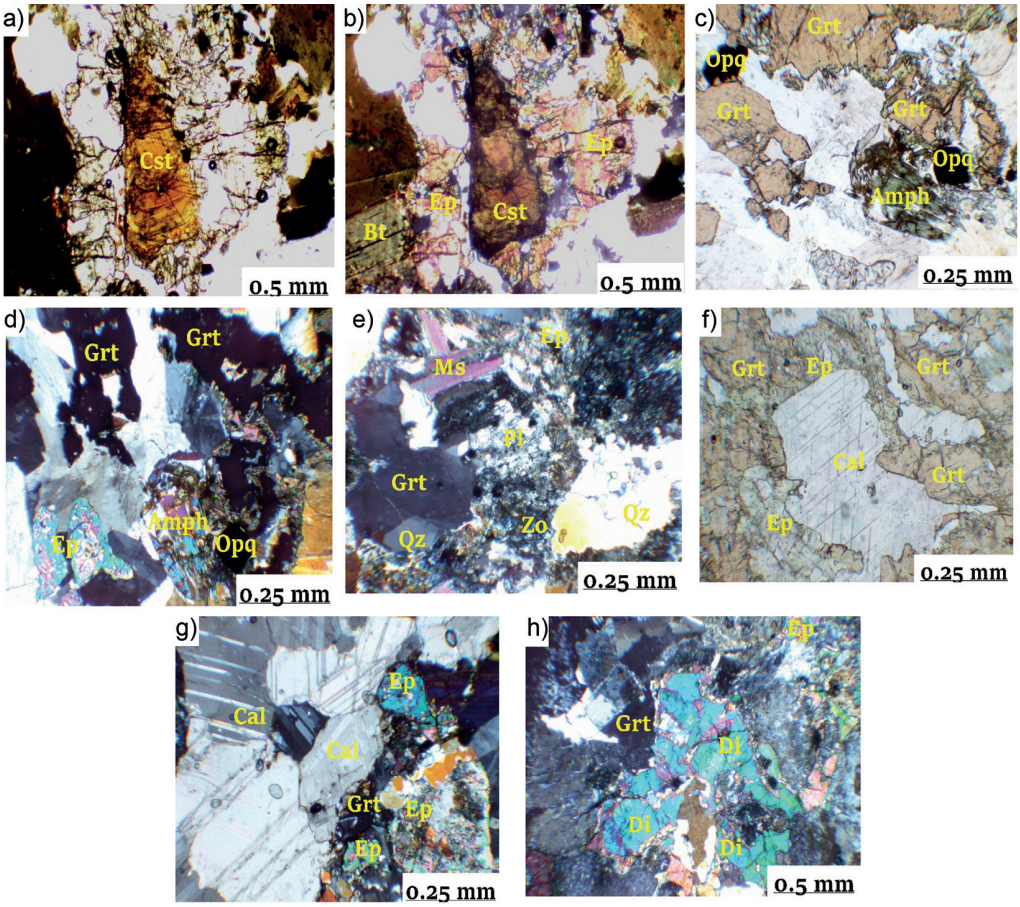

Fig. 2. A microscopic image of the related igneous rocks and skarn minerals: cassiterite and biotite are visible in biotite granite (analyzer out) (a); cassiterite, epidote, and biotite are visible in biotite granite (analyzer in) (b); amphibole, garnet, and opaque minerals are visible in skarn mineralization (analyzer out) (c); garnet and amphibole in skarn (analyzer in) (d); quartz, plagioclase, muscovite, zoisite, and garnet in skarn (analyzer in) (e); skarn consists dominated by garnet, epidote, and calcite (analyzer out) (f); shows the contact metamorphism between marble and skarn mineralization, marble represented by crystal of calcite and skarn by epidote and garnet (analyzer in) (g); diopside minerals abundant in skarn (analyzer in) (h). Mineral abbreviations: Qz, quartz; Pl, plagioclase; Ms, muscovite; Cal, calcite; Bt, biotite; Amp, amphibole; Ep, epidote; Di, diopside; Cst, cassiterite; Zo, zoisite; Opq, opaque mineral

Рис. 2. Микроизображение смежных вулканических пород и минералов скарна: касситерит и биотит, различимые в биотитовом граните (внутренний анализ) (а); касситерит, эпидот и биотит в биотитовом граните (внутренний анализ) (б); амфибол, гранат и опаковые минералы в скарновой минерализации (внешний анализ) (в); гранат и амфибол в скарне (внутренний анализ) (г); кварц, плагиоклаз, мусковит, цоизит и гранат в скарне (внутренний анализ) (д); скарн с преобладанием граната, с эпидотом и кальцитом (внешний анализ) (е); контактный метаморфизм между мрамором и скарновой минерализацией, мрамор представлен кристаллом кальцита, а скарн — эпидотом и гранатом (внутренний анализ) (ж); диопсид, обильно присутствующий в скарне (внутренний анализ) (з). Условные обозначения минералов: Qz — кварц; Pl — плагиоклаз; Ms — мусковит; Cal — кальцит; Bt — биотит; Amp — амфибол; Ep — эпидот; Di — диопсид; Cst — касситерит; Zo — цоизит; Opq — опаковый минерал

The results and discussion

Petrographic investigation of intrusion rocks and skarn mineralization

Microgranite shows a medium- to coarse-grained texture and is composed primarily of quartz (15–25%), alkali feldspar (20–50%), plagioclase (20–40%), and biotite (5–10%).

The biotite granite contains mainly quartz (15–20%), plagioclase (35–55%), k-feldspar (15–35%), and biotite (5–15%).

Leucogranite minerals are quartz (30–35%), plagioclase (20–30%), K-feldspar (10–15%), and biotite (0–5%). The leucogranite is characterized by deformed plagioclase lamellae, and most of the plagioclase is altered.

Diorite minerals are quartz (5–10%), plagioclase (50–55%), K-feldspar (5–10), biotite (15–35%), and amphibole (0–5%). Secondary minerals: chlorite, epidote, and sericite. Most of the granitic rocks show accessory minerals represented by apatite, monazite, and cassiterite (Fig. 2, *a, b*). The structure of the rock is fine-grained and hypidiomorphic.

Skarn mineralization in thin section is characterized mainly by garnet, epidote, pyroxene, and amphibole (Fig. 2, *c–h*). The petrography investigation shows garnet intergrowth over epidote (Fig. 2, *f*). Microcline, muscovite, clinoziosite, plagioclase, quartz, calcite, and scheelite are also present in the mineralization. Mineralization occasionally reveals opaque minerals. The metasomatic process results in altered minerals in skarn mineralization.

Skarn shows different types of metamorphic and metasomatic minerals, suggesting intensive hydrothermal activity. Garnet and pyroxene minerals occur in the early stage of metasomatic when magma intruded the carbonate rocks that indicate prograde stage, whereas the presence of epidote, quartz, calcite and chlorite is

Table 1

Whole rock major compositions of skarn and granitoids rocks in Dark Kingdom «Marble deposit»

Составы скарнов и гранитоидов в массиве пород, слагающих месторождение мрамора «Темное королевство» (Dark Kingdom)

Analyzed Sample	SKT1	SKT2	MG1	MG2	MG3	LG1	LG2	LG3	BG1	BG3	D1
Rock type	karn		granite								diorite
Major oxides wt.%											
Na_2O	0.48	4.01	5.29	4.89	4.94	5.98	5.84	5.63	4.42	5.33	5.34
MgO	0.14	1.75	0.53	0.46	0.75	0.19	0.1	0.08	0.82	1.65	3.95
Al_2O_3	11.37	14.36	14.62	15.17	14.82	12.71	12.89	13.84	15.38	17.3	17.95
SiO_2	45.85	47.71	70.64	70.45	69.85	73.43	76.17	74.62	69.52	59.54	52.89
K_2O	0.05	0.41	3.47	3.43	3.45	2.44	2.47	3.61	3.67	3.5	2
CaO	26.58	17.33	2.06	1.81	1.99	2.77	0.95	0.53	2.23	4.81	6.37
TiO_2	0.56	0.46	0.23	0.22	0.21	0.02	0.03	0.02	0.39	0.66	1.18
MnO	0.412	0.139	0.043	0.037	0.038	0.015	0.022	0.007	0.033	0.093	0.096
Fe_2O_3	7.56	5.28	1.93	1.82	1.98	0.28	0.52	0.36	2.51	5.02	7.61
P_2O_5	0.11	0.44	0.09	0.07	0.07	0.01	0.02	0.02	0.14	0.28	0.53

principal characteristic of retrograde alteration [21, 22].

Geochemistry of skarn mineralization

The major elemental compositions of skarn mineralization are summarized in Table 1. In comparison to the relatively high SiO_2 content of granitic rocks, skarn has a low SiO_2 content ranging from 47.71 to 45.85 wt.%. The high CaO content of skarn (26.58 – 17.33) reflects the carbonate characteristic. Unlike granite, which is silica-enriched with SiO_2 ranging from (76.14 to 59.54 weight percent), diorite has an intermediate SiO_2 chemical composition (52.89 weight percent). Granitoids, a type of rock, have high total alkalis (K_2O+Na_2O = 7.34 – 9.24 wt.%), moderate K_2O/Na_2O ratios ranging from (0.83 – 0.37), and very low to low CaO (0.53 – 6.37 wt.%) contents, as well as P_2O_5 (0.01 – 0.53 wt.%) contents. Most sample's analyses reflect a low LOI (loss on ignition), with values ranging from 0.64 to 2.13 wt.%. In comparison to igneous rocks, skarn mineralization has a low silica content, a high CaO content, and a low concentration of K_2O.

Granite, high-K calc-alkaline and metaluminous I-type granites are identified in the Syrostan massive complex (Fig. 3, *a, b*). CIWP norm for granitic rocks Table 2 displays quartz ranging from 5 to 30 wt.%, high albite and moderate orthoclase content, ranging between 37.5 and 50.5 and 14.5 and 21.5, respectively.

Granitic samples show corundum (ranging from 0 to 0.5 wt.%) < 1 in the most granite rocks, suggesting I-type granites that contain corundum less than 1 [23, 24].

In summary, determining the type of granite is important for understanding their feature [25]. Despite the skarn mineralization occurs in the contact between the diorite and carbonate rocks, many deposits worldwide are associated with peralkaline granite, whereas W, Mo, and Sn deposits are associated with metaluminous and I-type granite [26 – 28]. However, the presence of a granitoid intrusion with skarn mineralization at deep horizons that can produce ore mineralization can be predicted.

Skarn mineralization shows low LILE in comparison to granite and diorite, particularly very low content of K and Sr com-

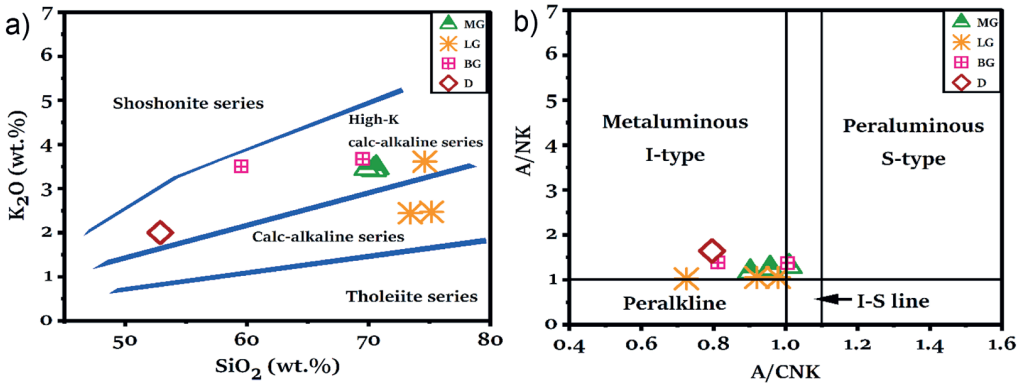

Fig. 3. Plots of granite samples: SiO_2 versus K_2O diagram [34], demonstrating the presence granitoid rocks among the high-k calc alkaline series (a); Al saturation index A/CNK molar [$Al_2O_3/(CaO+Na_2O+K_2O)$] versus A/NK molar ($Al_2O_3/(Na_2O+K_2O)$] diagram, showing the samples as metaluminous to peraluminous (b)

Рис. 3. Диаграммы, полученные для образцов гранита: взаимоотношение SiO_2 и K_2O [34], заметно демонстрирующее наличие гранитоидных пород среди высоко калийно-щелочных слоев (а); индекс насыщения Al (A)/CNK молярный [$Al_2O_3/(CaO+Na_2O+K_2O)$] в зависимости от A/NK молярный ($Al_2O_3/(Na_2O+K_2O)$] для образцов от мета-алюминиевых пералюминиевых (б)

Table 2

CIWP norm for investigated samples
Норма катионов CIWP для исследуемых образцов

	MG1	MG2	MG3	LG1	LG2	LG3	BG1	BG3	D1
Mineral					wt.%				
Q	22.45	24.5	23.05	25.95	31.25	27.01	24.15	5.15	0
C	0	0.23	0	0	0	0	0.5	0	0
Or	20.5	20.3	20.5	14.5	14.5	21.5	21.5	20.6	11.8
Ab	44.7	41.5	41.8	50.5	49.5	47.6	37.4	45.1	45.2
An	5.8	8.5	8	0.63	1.66	1.83	10.15	12.94	19.10
Di	2.4	0	0.59	1.02	0.53	0.43	0	5.57	3.85
Wo	0	0	0	4.89	0.92	0.03	0	0	0
Hy	0.2	1.14	1.594	0	0	0	2.04	1.53	1.67
Ol	0	0	0	0	0	0	0	0	4.47
Il	0.09	0.07	0.08	0.03	0.04	0.02	0.071	0.3	0
Hm	1.9	1.82	1.98	0.28	0.52	0.36	2.51	5.02	7.6
Tn	0.5	0	0.41	0.008	0.02	0.03	0	1.4	2.89
Ru	0	0.17	0	0	0	0	0.35	0	0
Ap	0.2	0.16	0.16	0.02	0.05	0.05	0.33	0.66	1.25
Py	0	0	0	0	0	0	0	0	0.16
Sum	98.9	98.4	98.11	97.85	99.02	98.73	99.13	98.20	98.02

pared to granite rocks (Fig. 4, *a*), indicating high mobility of these elements during the metasomatic process and the formation of new minerals [29, 30]. Investigated skarn samples contain concentrations of Ta of 2.4 and 2.3 ppm, while Hf concentrations in skarn are 2.7 and 2.5 ppm, respectively, higher than the concentrations of these elements in diorite and granites (Fig. 4, *b*). These findings suggest a high content of HSFE in skarn mineralization in comparison to granite rocks [31], but less than HSFE in diorite.

On the plot of REE primitive mantle in granite, diorite, and skarn (Fig. 4, *c*), the studied samples show LREE enrichment in granite and diorite samples relative to skarn.

On the contrary, investigated samples display HREE enrichment in skarn relative to diorite and granite samples.

Several factors influence the behavior of trace and rare earth elements (REE) in skarn mineralization, including fluid composition and temperature, host rock mineralogy and chemistry, and metamorphism degree. Depending on the metamorphic conditions, REE can be enriched or depleted in skarn minerals and host rocks.

The concentration of Nb in skarn mineralization ranges from 25 to 27 ppm, while diorite has a concentration of about 21 ppm and granitic rocks have a concentration of 9—15 ppm. indicating the presence of high Nb anomalies in skarn.

Sr, K, Rb, and Ba have low concentrations in skarn comparing to igneous rocks, indicating that these elements are highly mobile during fluid-rock interaction and mineral precipitation.

Trace element concentrations such as Cu, Pb, and Mo in skarn mineralization

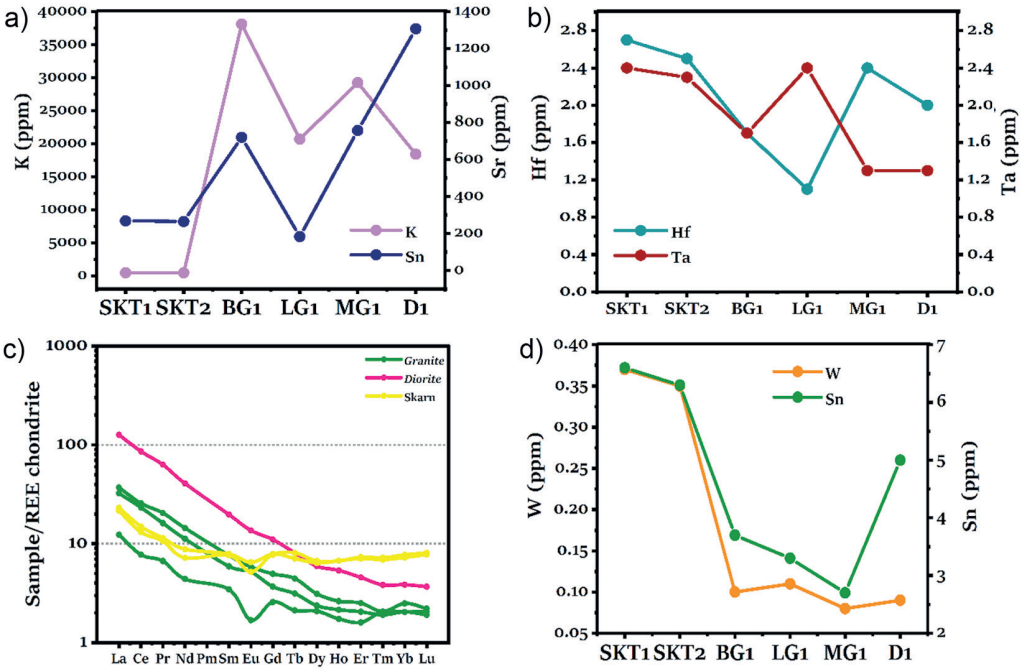

Fig. 4. Plot of trace and rare elements of skarn and granite samples shows the different concentration of K and Sr (a); displays various concentration of Hf and Ta (b); spider plot of REE primitive mantle demonstrate concentration of HREE & LREE in granites and skarn mineralization [35] (c); shows high concentration of W & Sn in skarn samples relative to granites (d). Abbreviations: BG, biotite granite; LG, leucogranite; MG, microgranite; D, diorite; SKT, skarn

Рис. 4. Примесные и редкие элементы в образцах скарна и гранита: концентрации K и Sr (а); концентрации Hf и Ta (б); диаграмма-паук примитивной мантии РЗЭ, демонстрирующая концентрации тяжелых и легких редкоземельных металлов в гранитах и скарновой минерализации [35] (в); высокие концентрации W и Sn по сравнению с гранитом в образцах скарна (г). Условные обозначения: BG — биотитовый гранит; LG — лейкогранит; MG — микрогранит; D — диорит; SKT — скарн

are low in comparison to igneous rocks, indicating that these elements are mainly concentrated in the mineral assemblages governed by fluid chemistry, temperature, and pressure during skarn formation, including sulfides like pyrite, chalcopyrite, and sphalerite.

W concentrations in skarn investigated samples ranged from 0.35 to 0.37 ppm, with Sn concentrations ranging from 6.3 to 6.6 ppm. whereas the concentration of W in igneous rocks ranges from 0.09 to 0.11 ppm, and the concentration of Sn ranges from 2.7 to 3.7 ppm. However, the concentration of Sn in diorite is 5 ppm. The skarn samples investigated display high W and Sn concentrations relative to granite and diorite (Fig. 4, *d*). These results indicate the possibility of W and Sn in skarn mineralization [32, 33].

Because of their preferential incorporation into specific minerals during metamorphism, REE are generally enriched in skarn minerals such as garnet, epidote, vesuvianite, and titanite compared to host rocks. The chemistry of the fluids, which tend to transport REE into skarns, where they are incorporated into new minerals, largely controls this behavior.

The geochemistry of skarn mineralization in the contact with diorite in the Syrostan massive would provide valuable

Table 3

Trace and other rare elements concentration in skarn and rocks

Концентрации примесных и других редких элементах в скарнах и других породах

Sample	SKT1	SKT2	BG1	LG1	MG1	D1
Trace & REE ppm						
K	438	447	38 103	20 671	29 248	18 391
Ti	3234	3267	2812	130	1278	7355
Be	1.1	1.3	2.6	3.1	1.4	2
Sc	5.7	5.4	3.4	0.47	1.8	10
V	299	287	39	3.7	18	115
Cr	8	9	6.8	<1,0	3.2	149
Co	5.6	5.3	5.2	0.64	2.5	24
Ni	15	13	5.9	2	2.7	56
Cu	15	13	27	19	13	123
Zn	39	35	53	3.6	43	93
Ga	30	28	24	12	21	24
As	16	14	18	6	9	28
Se	8	6	<0,5	<0,5	<0,5	31
Rb	0.7	0.6	82	36	68	58
Sr	268	265	720	183	757	1307
Y	34	32	10	7	9	19
Nb	27	25	15	13	9	21
Mo	5.7	5.3	9	11	7	7
Ag	0.35	0.29	0.41	0.16	0.56	0.73
Cd	1.5	1.2	<0,05	<0,05	<0,05	0.07
Sn	6.6	6.3	3.7	3.3	2.7	5
Sb	0.17	0.15	0.17	0.17	0.12	0.12
Te	<0,3	<0,3	<0,3	<0,3	<0,3	<0,3
Cs	0.05	0.04	1.5	0.33	1.1	1.3
Ba	57	53	1150	211	1130	862
La	15	14	24	8	21	82
Ce	25	22	43	13	39	144
Pr	2.9	2.7	5.2	1.7	4.1	16
Nd	11	9	18	5.5	14	51
Sm	3.2	3.1	3.1	1.4	2.4	8
Eu	1	1	0.9	0.26	0.8	2.1
Gd	4.3	4.2	2.7	1.4	2	6
Tb	0.8	0.7	0.44	0.21	0.31	0.8
Dy	4.5	4.3	2.1	1.4	1.6	4
Ho	1	1	0.39	0.26	0.32	0.8
Er	3.2	3.1	1.1	0.7	0.9	2

Tm	0.49	0.47	0.14	0.14	0.13	0.26
Yb	3.4	3.2	1.1	0.9	0.9	1.7
Lu	0.55	0.53	0.15	0.14	0.13	0.25
Hf	2.7	2.5	1.7	1.1	2.4	2
Ta	2.4	2.3	1.7	2.4	1.3	1.3
W	0.37	0.35	0.1	0.11	<0,08	0.09
Re	<0.01	<0.01	<0,01	<0.01	<0.01	<0.01
Pb	5.7	5.4	19	9	16	10
Bi	0.5	0.4	0.033	<0,01	<0,01	0.035
Th	5.5	5.3	6.2	7	6.5	11
U	3	2	1.7	0.7	1.2	1.7
Tl	<0,01	<0,01	0.41	0.14	0.28	0.32
Zr	58	56	65	25	103	105

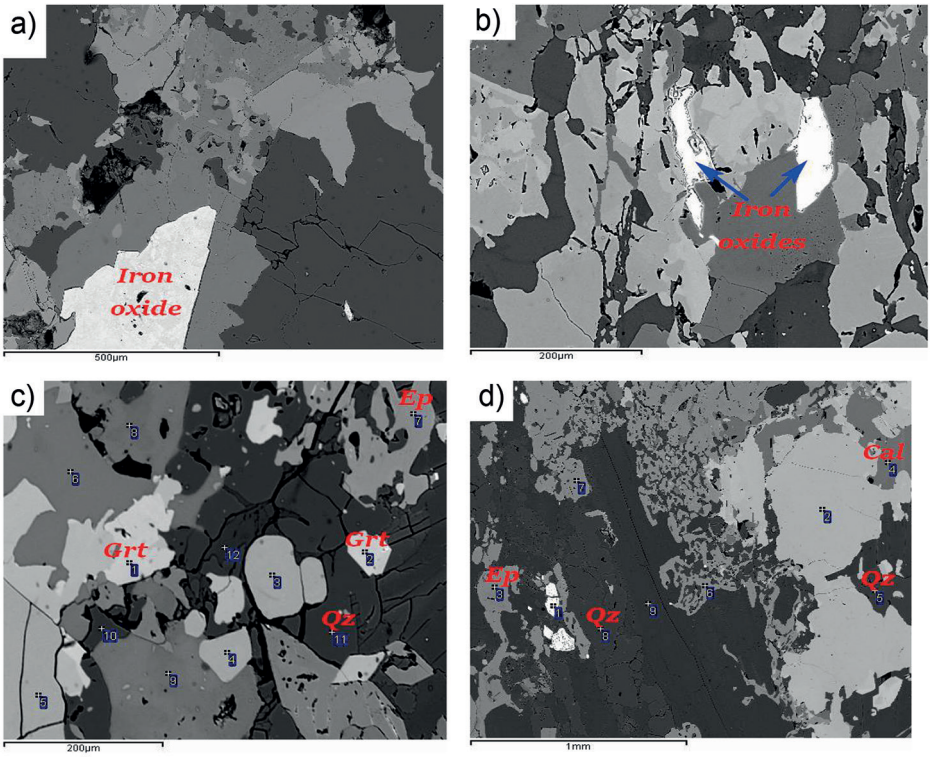

Fig. 5. BSE images for mineral of skarn mineralization BSE image show iron oxide minerals (a and b); BSE image garnet-magnetite-epidote-quartz phase (c); BSE image shows the presence of epidote, quartz, and calcite (d). Mineral abbreviations: Qz, quartz; Cal, calcite; Ep, epidote; Grt, garnet

Рис. 5. Изображение скарновой минерализации в отраженных электронах: минералы оксидов железа (а и б); гранат–магнетит–эпидот–кварцевая фаза (в); эпидот, кварц и кальцит (г). Условные обозначения: Qz — кварц; Cal — кальцит; Ep — эпидот; Grt — гранат

Table 4

Electron microprobe analysis of iron oxide for skarn mineralization

Результаты электронно-зондового микроанализа оксидов железа скарновой минерализации

Na	0.31	0	0.19	0.12	0	0.09	0.08	0.19	0.23
Mg	0.24	0.19	0.09	0.09	0.08	0.04	0	0.11	0
Al	0.18	0.12	0.6	0.04	0.02	0.07	0	0.26	0.07
Si	1.79	1.68	6.8	1.42	1.81	1.92	1.95	0.07	1.83
P	0.19	0.2	0.1	0	0	0.07	0.06	0.07	0.21
K	0	0.02	0.09	0.02	0	0.02	0	0.05	0
Ca	0.47	0.34	0.87	0.41	0.41	0.51	0.5	1.06	0.55
Ti	0	0	0	0	0.05	0.11	0	2.42	0
V	0.03	0.08	0	0	0.02	0	0.03	0.52	0
Cr	0.03	0.02	0.04	0.07	0.02	0	0	0	0
Mn	0.03	0	0.07	0.06	0.05	0.12	0.19	0.11	0.05
Fe	57.72	56.4	47.11	54.74	55.79	55.73	54.28	61.66	58.15
Co	0.75	0.59	0.4	0.44	0.63	0.43	0.65	0.73	0.4
Ni	0.23	0.17	0	0.1	0.16	0.17	0	0.13	0.11
Cu	0	0	0.15	0.13	0.07	0	0	0.16	0
Zn	0	0	0.25	0.28	0	0.09	0.09	0.11	0.23
O	19.75	18.98	22.65	17.9	18.59	18.86	18.35	21	19.58
Total	81.72	78.79	79.42	75.82	77.7	78.23	76.18	88.65	81.4

information about mineralization, and element concentration, in addition the geochemistry of granite and diorite will improve well insight related to magma evolution.

Additionally, this research is insufficient with regard to geochemical analysis and the mineral chemistry of skarn mineralization. Hence, more research will be focused on in situ major and trace element analysis and mineral chemistry in order to decipher the mineralization content, metallogeny, and implications for the emplacement of the possible mineralization potential.

Mineral chemistry of skarn mineralization and ore minerals

The investigation of a microprobe for one sample of skarn mineralization reveals that the skarn is enriched in iron oxide, most likely magnetite (Fig. 5, *a, b*). These findings imply the potential for iron oxide mineralization in the deep horizon skarn with intrusions.

According to many research magnetite and iron oxide deposits are hosted in carbonate rocks and formed during garnet-magnetite-epidote-quartz phase, that supported by the petrography survey and microprobe analysis for the same sample, that shows garnet, epidote, and quartz minerals (Fig. 5, *c*).

In skarn mineralization containing iron oxides, the Co/Ni ratios in the iron oxide (2.5 to 5.5) demonstrate the hydrothermal impact on the magmatic source. As a result, fluctuating Co/Ni ratios show interactions between the magma and host rock during repeated alteration stages [36].

Garnet and pyroxene minerals are early metasomatic stage minerals that indi-

cate a prograde stage of alteration. Garnet is Al bearing andradite. The presence of epidote, quartz, calcite, and chlorite in an exoskarn distinguishes retrograde alteration (Fig. 5, *d*) [37].

Conclusion

This research has studied the geochemistry and petrography of Skarn mineralization, and the results of this investigation show that:

1. Petrography investigation revealed that skarn mineralization in the contact between diorite and carbonate rocks is dominated by garnet, epidote, amphibole, and pyroxene. Cassiterite occurs in biotite granite.

2. Syrostan massive contains High-K calc-alkaline granite and I-type with diorite, which crossed the marble as veins following the tectonic joints.

3. Skarn studied samples revealed enrichment in HREE relative to LREE in granites and diorite.

4. Skarn mineralization appeared to have higher concentrations of Mo, W, Sn, Ta, and Nb.

5. Co/Ni ratios in iron oxide show interactions between the magma and host rock during repeated alteration stages.

СПИСОК ЛИТЕРАТУРЫ

1. *Zhang Z., Xie G., Thompson J.* Skarn mineralogy and in-situ LA—ICP—MS U—Pb geochronology of wolframite for the Caojiaba tungsten deposit, southern China: Implications for a reduced tungsten skarn deposit // Ore Geology Reviews. 2022, vol. 147, article 104981. DOI: 10.1016/j.oregeorev.2022.104981.

2. *Case G. N. D.*, *Graham G. E.*, *Marsh E. E.*, *Taylor R. D.*, *Green C. J.*, *Brown P. J.*, *Labay K. A.* Tungsten skarn potential of the Yukon-Tanana Upland, eastern Alaska, USA—A mineral resource assessment // Journal of Geochemical Exploration. 2020, vol. 232, article 106700. DOI: 10.1016/j.gexplo.2020.106700.

3. *Meinert L. D.* Skarns and skarn deposits // Geoscience Canada. 1992, vol. 19, no. 4, pp. 145—162.

4. *Yıldırım E.*, *Yıldırım N.*, *Dönmez C.*, *Koh S. M.*, *Günay K.* Mineralogy, rare earth elements geochemistry and genesis of the Keban-West Euphrates (Cu-Mo)-Pb-Zn skarn deposit (Eastern Taurus metallogenic belt, E Turkey) // Ore Geology Reviews. 2019, vol. 114, article 103102. DOI: 10.1016/j.oregeorev.2019.103102.

5. *Lemière B.* A review of pXRF (field portable X-ray fluorescence) applications for applied geochemistry // Journal of Geochemical Exploration. 2018, vol. 188, pp. 350—363. DOI: 10.1016/j.gexplo.2018.02.006.

6. *Lemière B.*, *Uvarova Y. A.* New developments in field-portable geochemical techniques and onsite technologies and their place in mineral exploration // Geochemistry: Exploration, Environment, Analysis. 2020, vol. 20, no. 2, pp. 205—216. DOI: 10.1144/geochem2019-044.

7. *Richards M. J.* Realising the potential of portable XRF for the geochemical classification of volcanic rock types // Journal of Archaeological Science. 2019, vol. 105, pp. 31—45. DOI: 10.1016/j.jas.2019.03.004.

8. *Belogub E. V.*, *Melekestseva I. Yu.*, *Novoselov K. A.*, *Zabotina M. V.*, *Tret'yakov G. A.*, *Zaykov V. V.*, *Yuminov A. M.* Listvenite-related gold deposits of the South Urals (Russia). A review // Ore Geology Reviews. 2017, vol. 85, pp. 247—270. DOI: 10.1016/j.oregeorev.2016.11.008.

9. *Herrington R. J.*, *Plotinskaya O. Y.*, *Maslennikov V. V.*, *Tessalina S. G.* An overview of mineral deposits in the Urals // Ore Geology Reviews. 2017, vol. 85, pp. 1—3. DOI: 10.1016/j.oregeorev.2016.12.016.

10. *Знаменский С. Е.*, *Анкушева Н. Н.*, *Веливецкая Т. А.*, *Шанина С. Н.* Состав и источники минералообразующих флюидов Орловского орогенного месторождения золота (Южный Урал) // Геология и геофизика. — 2017. — Т. 58. — № 9. — С. 1070—1079. DOI: 10.1016/j.rgg.2017.08.003.

11. *Brusnitsyn A. I.*, *Zhukov I. G.* Manganese deposits of the Devonian Magnitogorsk palaeovolcanic belt (Southern Urals, Russia) // Ore Geology Reviews. 2012, vol. 47, pp. 42—58. DOI: 10.1016/j.oregeorev.2012.01.003.

12. *Wang C., Li J., Wang K., Yu Q., Liu G.* Geology, fluid inclusion, and stable isotope study of the skarn-related Pb—Zn (Cu—Fe—Sn) polymetallic deposits in the southern Great Xing'an Range, China: implications for deposit type and metallogenesis // Arabian Journal of Geosciences. 2018, vol. 11, no. 5. DOI: 10.1007/s12517-018-3417-6.

13. *Niu X., Shu Q., X. Kai, Yuan S., Wei L., Zhang Y., Yu F., Zeng Q., Ma Sh.* Evaluating Sn mineralization potential at the Haobugao skarn Zn-Pb deposit (NE China) using whole-rock and zircon geochemistry // Journal of Geochemical Exploration. 2022, vol. 234, article 106938. DOI: 10.1016/j.gexplo.2021.106938.

14. *Soloviev S. G.*, *Kryazhev S. G.*, *Dvurechenskaya S. S.*, *Uyutov V. I.* Geology, mineralization, fluid inclusion, and stable isotope characteristics of the Sinyukhinskoe Cu-Au skarn deposit, Russian Altai, SW Siberia // Ore Geology Reviews. 2019, vol. 112, article 103039. DOI: 10.1016/j.oregeorev.2019.103039.

15. *Белковский А. И., Нестеров А. Р.* Минералогия марганцевых скарнов, генетически связанных со щелочными гранитами (на примере Уфимского рудника, Южный Урал) // Литосфера. — 2018. — Т. 18. — № 1. — С. 127—132. DOI: 10.24930/1681-9004-2018-18-1-127-132.

16. *Ibrahim M. A. E.*, *Kotelnikov A. E.* Geological and Geochemical exploration methods for mineral resources (skarn deposits and rare earth elements) // Известия Уральского государственного горного университета. — 2022. — № 2(66). — С. 7—15. DOI: 10.21440/2307-2091-2022-2-7-15.

17. *Ковалев С.Г., Ковалев С.С.* Ti-Fe-Cr шпинелиды в дифференцированных (расслоенных) комплексах западного склона Южного Урала: видовое разнообразие и условия формирования // Записки Горного института. — 2022. — Т. 255. — С. 476—492. DOI: 10.31897/PMI.2022.54.

18. *Georgievskiy A. F.*, *Bugina V. M.*, *Kotelnikov A. E.*, *Georgievskiy A. A.*, *Mahinja E.*, *Gamilton Z. A.* Vein-rock in the Dark kingdom Marble Deposit (South Ural) and their possible connection with gold ore mineralization // IOP Conference Series: Earth And Environmental Science. 2021, vol. 666, no. 2, article 022024. DOI: 10.1088/1755-1315/666/2/022024.

19. *Zaykov V. V.*, *Melekestseva I. Y.*, *Zaykova E. V.*, *Kotlyarov V. A.*, *Kraynev Y. D.* Gold and platinum group minerals in placers of the South Urals: Composition, microinclusions of ore minerals and primary sources // Ore Geology Reviews. 2017, vol. 85, pp. 299—320. DOI: 10.1016/j.oregeorev.2016.10.001.

20. *Maslennikov V. V.*, *Maslennikova S. P.*, *Large R. R.*, *Danyushevsky L. V.* Study of trace element zonation in vent chimneys from the Silurian Yaman-Kasy volcanic-hosted massive sulfide deposit (Southern Urals, Russia) using laser ablation-inductively coupled plasma mass spectrometry (LA-ICPMS) // Economic Geology and the Bulletin of the Society of Economic Geologists. 2009, vol. 104, no. 8, pp. 1111—1141. available at: http://www.epa.gov/glnpo/atlas/gl-fact1.html. DOI: 10.2113/gsecongeo.104.8.1111.

21. *Jiang J., Gao S., Zheng Y., Lentz D. R., Huang J., Liu J., Tian K., Jiang X.* Geological, geochemical, and mineralogical constraints on the genesis of the polymetallic Pb-Zn-Rich Nuocang Skarn Deposit, Western Gangdese, Tibet // Minerals. 2020, vol. 10, article 839. DOI: 10.3390/min10100839.

22. *Hassanpour S., Rajabpour S.* Magmatic — hydrothermal evolution of the Anjerd Cu skarn deposit, NW Iran: Perspectives on mineral chemistry, fluid inclusions and stable isotopes // Ore Geology Reviews. 2019, vol. 117, article 103269. DOI: 10.1016/j.oregeorev.2019.103269.

23. *Ahnaf J. S.*, *Patonah A.*, *Permana H.* Petrogenesis of volcanic arc granites from Bayah Complex, Banten, Indonesia // Journal of Geoscience Engineering Environment and Technology. 2019, vol. 4, pp. 104—115. DOI: 10.25299/jgeet.2019.4.2.3171.

24. *Chappell B. W.*, *Bryant C. J.*, *Wyborn D.* Lithos peraluminous I-type granites // Lithos. 2012, vol. 153, pp. 142—153. DOI: 10.1016/j.lithos.2012.07.008.

25. *Alaminia Z., Tadayon M., Finger F., Lentz D. R., Waitzinger M.* Analysis of the in fi ltrative metasomatic relationships controlling skarn mineralization at the Abbas-Abad Fe-Cu Deposit, Isfahan, north Zefreh Fault , Central Iran // Ore Geology Reviews. 2020, vol. 117, article 103321. DOI: 10.1016/j.oregeorev.2020.103321.

26. *Helmy H. M.*, *Kaindl R., Shibata T.* Genetically related Mo-Bi-Ag and U-F mineralization in A-type granite, Gabal Gattar, Eastern Desert, Egypt // Ore Geology Reviews. 2014, vol. 62, pp. 181—190. DOI: 10.1016/j.oregeorev.2014.03.008.

27. *Song S., Mao J., Xie G., Su Q., Jian W., Ouyang Y.* Deciphering deep-seated, highly fractionated, and reduced granitic magma systems associated with world-class scheelite skarn ores. A case study of the Zhuxi deposit, South China // Ore Geology Reviews. 2022, vol. 149, article 105084. DOI: 10.1016/j.oregeorev.2022.105084.

28. *Soloviev S. G.*, *Kryazhev S. G.*, *Dvurechenskaya S. S.*, *Kryazhev V. S.*, *Emkuzhev M. S.*, *Bortnikov N. S.* The superlarge Tyrnyauz skarn W-Mo and stockwork Mo(-W) to Au(-Mo, W, Bi, Te) deposit in the Northern Caucasus, Russia: Geology, geochemistry, mineralization, and fluid inclusion characteristics // Ore Geology Reviews. 2021, vol. 138, article 104384. DOI: 10.1016/j.oregeorev.2021.104384.

29. *Zhang W., Jiang S. Y., Gao T., Ouyang Y., Zhang D.* The effect of magma differentiation and degassing on ore metal enrichment during the formation of the world-class Zhuxi W-Cu skarn deposit: Evidence from U-Pb ages, Hf isotopes and trace elements of zircon, and whole-rock geochemistry // Ore Geology Reviews. 2020, vol. 127, article 103801. DOI: 10.1016/j.oregeorev.2020.103801.

30. *Maghraoui M. El., Joron J. L., Raimbault L., Treuil M.* Element mobility during metasomatism of granitic rocks in the Saint-Chély d'Apcher area (Lozère, France) // Environment International. 2002, vol. 28, no. 5, pp. 349—357. DOI: 10.1016/S0160-4120(02)00036-3.

31. *Somarin A. K., Moayyed M.* Granite- and gabbrodiorite-associated skarn deposits of NW Iran // Ore Geology Reviews. 2002, vol. 20, no. 3—4, pp. 127—138. DOI: 10.1016/S0169-1368(02)00068-9.

32. *Goryachev N. A.*, *Shpikerman V. I.*, *Church S. E.*, *Gvozdev V. I.* Calcic skarn ore deposits of the North-East Russia // Ore Geology Reviews. 2018, vol. 103, pp. 3—20. DOI: 10.1016/j.oregeorev.2018.03.024.

33. *Попов М. П.* Особенности редкометалльного оруденения и генетическая связь минеральных ассоциаций в восточном обрамлении Мурзинско-Адуйского антиклинория (Уральская изумрудоносная полоса) // Записки Горного института. — 2022. — Т. 255. — С. 337—348. DOI: 10.31897/PMI.2022.19.

34. *Peccerillo A.*, *Taylor S. R.*, Geochemistry of eocene calc-alkaline volcanic rocks from the Kastamonu area, Northern Turkey // Contributions to Mineralogy and Petrology. 1976, vol. 58, no. 1, pp. 63—81. DOI: 10.1007/BF00384745.

35. *McDonough W. F.*, *Sun S. S.* The composition of the Earth // Chemical Geology. 1995, vol. 120, no. 3—4, pp. 223—253. DOI: 10.1016/0009-2541(94)00140-4.

36. *Sipahi F.*, *Gücer M. A.*, *Eker Ç. S.* Geochemical composition of magnetite from different iron skarn mineralizations in NE Turkey: implication for source of ore-forming fluids // Arabian Journal of Geosciences. 2020, vol. 13, no. 2. DOI: 10.1007/s12517-019-5052-2.

37. *Zahedi A., Boomeri M., Nakashima K., Mackizadeh M. A., Ban M.*, *Lentz D. R.* Geochemical characteristics, origin, and evolution of ore-forming fluids of the Khut Copper Skarn deposit, west of Yazd in Central Iran // Resource Geology. 2014, vol. 64, no. 3, pp. 209—232. DOI: 10.1111/rge.12037. ГИАБ

REFERENCES

1. Zhang Z., Xie G., Thompson J. Skarn mineralogy and in-situ LA—ICP—MS U—Pb geochronology of wolframite for the Caojiaba tungsten deposit, southern China: Implications for a reduced tungsten skarn deposit. *Ore Geology Reviews*. 2022, vol. 147, article 104981. DOI: 10.1016/j.oregeorev.2022.104981.

2. Case G. N. D., Graham G. E., Marsh E. E., Taylor R. D., Green C. J., Brown P. J., Labay K. A. Tungsten skarn potential of the Yukon-Tanana Upland, eastern Alaska, USA — A mineral resource assessment. *Journal of Geochemical Exploration*. 2020, vol. 232, article 106700. DOI: 10.1016/j.gexplo.2020.106700.

3. Meinert L. D. Skarns and skarn deposits. *Geoscience Canada*. 1992, vol. 19, no. 4, pp. 145—162.

4. Yıldırım E., Yıldırım N., Dönmez C., Koh S. M., Günay K. Mineralogy, rare earth elements geochemistry and genesis of the Keban-West Euphrates (Cu-Mo)-Pb-Zn skarn deposit (Eastern Taurus metallogenic belt, E Turkey). *Ore Geology Reviews*. 2019, vol. 114, article 103102. DOI: 10.1016/j.oregeorev.2019.103102.

5. Lemière B. A review of pXRF (field portable X-ray fluorescence) applications for applied geochemistry. *Journal of Geochemical Exploration*. 2018, vol. 188, pp. 350—363. DOI: 10.1016/j.gexplo.2018.02.006.

6. Lemière B., Uvarova Y. A. New developments in field-portable geochemical techniques and on-site technologies and their place in mineral exploration. *Geochemistry: Exploration, Environment, Analysis*. 2020, vol. 20, no. 2, pp. 205—216. DOI: 10.1144/geochem2019-044.

7. Richards M. J. Realising the potential of portable XRF for the geochemical classification of volcanic rock types. *Journal of Archaeological Science*. 2019, vol. 105, pp. 31—45. DOI: 10.1016/j.jas.2019.03.004.

8. Belogub E. V., Melekestseva I. Yu., Novoselov K. A., Zabotina M. V., Tret'yakov G. A., Zaykov V. V., Yuminov A. M. Listvenite-related gold deposits of the South Urals (Russia). A review. *Ore Geology Reviews*. 2017, vol. 85, pp. 247—270. DOI: 10.1016/j.oregeorev.2016.11.008.

9. Herrington R. J., Plotinskaya O. Y., Maslennikov V. V., Tessalina S. G. An overview of mineral deposits in the Urals. *Ore Geology Reviews*. 2017, vol. 85, pp. 1—3. DOI: 10.1016/j.oregeorev.2016.12.016.

10. Znamenskii S. E., Ankusheva N. N., Velivetskaya T. A., Shanina S. N. Composition and sources of mineral-forming fluids of the Orlovka orogenic gold deposit (Southern Urals). *Russian Geology and Geophysics*. 2017, vol. 58, no. 9, pp. 1070—1079. [In Russ]. DOI: 10.1016/j.rgg.2017.08.003.

11. Brusnitsyn A. I., Zhukov I. G. Manganese deposits of the Devonian Magnitogorsk palaeovolcanic belt (Southern Urals, Russia). *Ore Geology Reviews*. 2012, vol. 47, pp. 42—58. DOI: 10.1016/j.oregeorev.2012.01.003.

12. Wang C., Li J., Wang K., Yu Q., Liu G. Geology, fluid inclusion, and stable isotope study of the skarn-related Pb—Zn (Cu—Fe—Sn) polymetallic deposits in the southern Great Xing'an Range, China: implications for deposit type and metallogenesis. *Arabian Journal of Geosciences*. 2018, vol. 11, no. 5. DOI: 10.1007/s12517-018-3417-6.

13. Niu X., Shu Q., X. Kai, Yuan S., Wei L., Zhang Y., Yu F., Zeng Q., Ma Sh. Evaluating Sn mineralization potential at the Haobugao skarn Zn-Pb deposit (NE China) using whole-rock and zircon geochemistry. *Journal of Geochemical Exploration*. 2022, vol. 234, article 106938. DOI: 10.1016/j.gexplo.2021.106938.

14. Soloviev S. G., Kryazhev S. G., Dvurechenskaya S. S., Uyutov V. I. Geology, mineralization, fluid inclusion, and stable isotope characteristics of the Sinyukhinskoe Cu-Au skarn deposit, Russian Altai, SW Siberia. *Ore Geology Reviews*. 2019, vol. 112, article 103039. DOI: 10.1016/j.oregeorev.2019.103039.

15. Belkovsky A. I., Nesterov A. R. Mineralogy of manganese skarns, genetically related to alkaline granites (on the example of the Ufa mine, Southern Urals). *Litosfera*, 2018, vol. 18, no. 1, pp. 127—132. [In Russ]. DOI: 10.24930/1681-9004-2018-18-1-127-132.

16. Ibrahim M. A. E., Kotelnikov A. E. Geological and Geochemical exploration methods for mineral resources (skarn deposits and rare earth elements). *News of Ural State Mining University*. 2022, no. 2(66), pp. 7—15. DOI: 10.21440/2307-2091-2022-2-7-15.

17. Kovalev S.G., Kovalev S.S. Ti-Fe-Cr spinels in layered (stratified) complexes of the western slope of the Southern Urals: species diversity and formation conditions. *Journal of Mining Institute*. 2022, vol. 255, no. 3, pp. 476—492. [In Russ]. DOI: 10.31897/PMI.2022.54

18. Georgievskiy A. F., Bugina V. M., Kotelnikov A. E., Georgievskiy A. A., Mahinja E., Gamilton Z. A. Vein-rock in the Dark kingdom Marble Deposit (South Ural) and their possible connection with gold ore mineralization. *IOP Conference Series: Earth And Environmental Science*. 2021, vol. 666, no. 2, article 022024. DOI: 10.1088/1755-1315/666/2/022024.

19. Zaykov V. V., Melekestseva I. Y., Zaykova E. V., Kotlyarov V. A., Kraynev Y. D. Gold and platinum group minerals in placers of the South Urals: Composition, microinclusions of ore minerals and primary sources. *Ore Geology Reviews*. 2017, vol. 85, pp. 299—320. DOI: 10.1016/j.oregeorev.2016.10.001.

20. Maslennikov V. V., Maslennikova S. P., Large R. R., Danyushevsky L. V. Study of trace element zonation in vent chimneys from the Silurian Yaman-Kasy volcanic-hosted massive sulfide deposit (Southern Urals, Russia) using laser ablation-inductively coupled plasma mass spectrometry (LA-ICPMS). *Economic Geology and the Bulletin of the Society of Economic Geologists*. 2009, vol. 104, no. 8, pp. 1111—1141. available at: http://www.epa.gov/glnpo/atlas/gl-fact1.html. DOI: 10.2113/gsecongeo.104.8.1111.

21. Jiang J., Gao S., Zheng Y., Lentz D. R., Huang J., Liu J., Tian K., Jiang X. Geological, geochemical, and mineralogical constraints on the genesis of the polymetallic Pb-Zn-Rich Nuocang Skarn Deposit, Western Gangdese, Tibet. *Minerals*. 2020, vol. 10, article 839. DOI: 10.3390/min10100839.

22. Hassanpour S., Rajabpour S. Magmatic — hydrothermal evolution of the Anjerd Cu skarn deposit, NW Iran: Perspectives on mineral chemistry, fluid inclusions and stable isotopes. *Ore Geology Reviews*. 2019, vol. 117, article 103269. DOI: 10.1016/j.oregeorev.2019.103269.

23. Ahnaf J. S., Patonah A., Permana H. Petrogenesis of volcanic arc granites from Bayah Complex, Banten, Indonesia. *Journal of Geoscience Engineering Environment and Technology*. 2019, vol. 4, pp. 104—115. DOI: 10.25299/jgeet.2019.4.2.3171.

24. Chappell B. W., Bryant C. J., Wyborn D. Lithos peraluminous I-type granites. *Lithos*. 2012, vol. 153, pp. 142—153. DOI: 10.1016/j.lithos.2012.07.008.

25. Alaminia Z., Tadayon M., Finger F., Lentz D. R., Waitzinger M. Analysis of the in fi ltrative metasomatic relationships controlling skarn mineralization at the Abbas-Abad Fe-Cu Deposit, Isfahan, north Zefreh Fault, Central Iran. *Ore Geology Reviews*. 2020, vol. 117, article 103321. DOI: 10.1016/j.oregeorev.2020.103321.

26. Helmy H. M., Kaindl R., Shibata T. Genetically related Mo-Bi-Ag and U-F mineralization in A-type granite, Gabal Gattar, Eastern Desert, Egypt. *Ore Geology Reviews*. 2014, vol. 62, pp. 181—190. DOI: 10.1016/j.oregeorev.2014.03.008.

27. Song S., Mao J., Xie G., Su Q., Jian W., Ouyang Y. Deciphering deep-seated, highly fractionated, and reduced granitic magma systems associated with world-class scheelite skarn ores. A case study of the Zhuxi deposit, South China. *Ore Geology Reviews*. 2022, vol. 149, article 105084. DOI: 10.1016/j.oregeorev.2022.105084.

28. Soloviev S. G., Kryazhev S. G., Dvurechenskaya S. S., Kryazhev V. S., Emkuzhev M. S., Bortnikov N. S. The superlarge Tyrnyauz skarn W-Mo and stockwork Mo(-W) to Au(-Mo, W, Bi, Te) deposit in the Northern Caucasus, Russia: Geology, geochemistry, mineralization, and fluid inclusion characteristics. *Ore Geology Reviews*. 2021, vol. 138, article 104384. DOI: 10.1016/j.oregeorev.2021.104384.

29. Zhang W., Jiang S. Y., Gao T., Ouyang Y., Zhang D. The effect of magma differentiation and degassing on ore metal enrichment during the formation of the world-class Zhuxi W-Cu skarn deposit: Evidence from U-Pb ages, Hf isotopes and trace elements of zircon, and whole-rock geochemistry. *Ore Geology Reviews*. 2020, vol. 127, article 103801. DOI: 10.1016/j.oregeorev.2020.103801.

30. Maghraoui M. El., Joron J. L., Raimbault L., Treuil M. Element mobility during metasomatism of granitic rocks in the Saint-Chély d'Apcher area (Lozère, France). *Environment International*. 2002, vol. 28, no. 5, pp. 349—357. DOI: 10.1016/S0160-4120(02)00036-3.

31. Somarin A. K., Moayyed M. Granite- and gabbrodiorite-associated skarn deposits of NW Iran. *Ore Geology Reviews*. 2002, vol. 20, no. 3—4, pp. 127—138. DOI: 10.1016/S0169-1368(02)00068-9.

32. Goryachev N. A., Shpikerman V. I., Church S. E., Gvozdev V. I. Calcic skarn ore deposits of the North-East Russia. *Ore Geology Reviews*. 2018, vol. 103, pp. 3—20. DOI: 10.1016/j.oregeorev.2018.03.024.

33. Popov M. P. Peculiarities of rare-metal mineralization and genetic relationship of mineral associations in the eastern rim of Murzinsko-Aduysky anticlinorium (the Ural Emerald Belt). *Journal of Mining Institute*. 2022, vol. 255, no. 3, pp. 337—348. [In Russ]. DOI: 10.31897/PMI.2022.19.

34. Peccerillo A., Taylor S. R., Geochemistry of eocene calc-alkaline volcanic rocks from the Kastamonu area, Northern Turkey. Contributions to Mineralogy and Petrology. 1976, vol. 58, no. 1, pp. 63—81. DOI: 10.1007/BF00384745.

35. McDonough W. F., Sun S. S. The composition of the Earth. *Chemical Geology*. 1995, vol. 120, no. 3—4, pp. 223—253. DOI: 10.1016/0009-2541(94)00140-4.

36. Sipahi F., Gücer M. A., Eker Ç. S. Geochemical composition of magnetite from different iron skarn mineralizations in NE Turkey: implication for source of ore-forming fluids. *Arabian Journal of Geosciences*. 2020, vol. 13, no. 2. DOI: 10.1007/s12517-019-5052-2.

37. Zahedi A., Boomeri M., Nakashima K., Mackizadeh M. A., Ban M., Lentz D. R. Geochemical characteristics, origin, and evolution of ore-forming fluids of the Khut Copper Skarn deposit, west of Yazd in Central Iran. *Resource Geology*. 2014, vol. 64, no. 3, pp. 209—232. DOI: 10.1111/rge.12037.

ИНФОРМАЦИЯ ОБ АВТОРАХ

Ибрахим Мохаммед Абдалла Альшариф[1] — аспирант,
научный сотрудник; ассистент,
e-mail: mohammedelsharif7@gmail.com,
ORCID ID: 0000-0002-5634-5695,
Котельников Александр Евгеньевич[1] — канд. геол.-минерал. наук,
доцент, директор Департамента, e-mail: kotelnikov-ae@rudn.ru,
ORCID ID: 0000-0003-0622-8391,

Георгиевский Алексей Федорович[1] — д-р геол.-минерал. наук,
доцент, e-mail: georgievskiy-af@rudn.ru,
ORCID ID: 0000-0003-4835-760X,
Ибрахим Самия Абдельрахман — канд. геол. наук,
директор Департамента геологии,
факультет Естественных наук, Хартумский университет,
Судан, e-mail: samiaibrahim125@gmail.com,
Мусаб Хассан[1] — аспирант, научный сотрудник;
ассистент, e-mail: musabeljah78@gmail.com,
ORCID ID: 0000-0003-2691-5703,
Анас Мухаммад Абкар Баби — аспирант, научный сотрудник;
ассистент, Факультет нефтегазовой геологии и полезных ископаемых,
Университет Бахри, Судан, e-mail: anasabaker@gmail.com,
ORCID ID: 0000-0003-2317-329X,
[1] Департамент недропользования и нефтегазового дела,
Инженерная академия, Российский университет дружбы народов.
Для контактов: Ибрахим Мохаммед Абдалла Альшариф,
e-mail: mohammedelsharif7@gmail.com.

INFORMATION ABOUT THE AUTHORS

Mohammed Abdalla Elsharif Ibrahim[1], Graduate Student,
Researcher; Assistant,
e-mail: mohammedelsharif7@gmail.com,
ORCID ID: 0000-0002-5634-5695,
A.E. Kotelnikov[1], Cand. Sci. (Geol. Mineral.),
Assistant Professor, Head of Department,
e-mail: kotelnikov-ae@rudn.ru,
ORCID ID: 0000-0003-0622-8391,
A.F. Georgievskiy[1], Dr. Sci. (Geol. Mineral.),
Assistant Professor, e-mail: georgievskiy-af@rudn.ru,
ORCID ID: 0000-0003-4835-760X,
Samia Abdelrahman Ibrahim, Dr. Sci. (Geol.),
Head of Geology Department,
Faculty of Natural Sciences, University of Khartoum, Sudan,
e-mail: samiaibrahim125@gmail.co
Musab Hassan[1], Graduate Student, Researcher;
Assistant, e-mail: musabeljah78@gmail.com,
ORCID ID: 0000-0003-2691-5703,
Anas Mohamed Abaker Babai, Graduate Student,
Researcher; Assistant, Faculty of Petroleum Geology
and Minerals, University of Bahri, Sudan,
e-mail: anasabaker@gmail.com,
ORCID ID: 0000-0003-2317-329X.
[1] Department of Mineral Development and Oil and Gas Engineering,
Academy of Engineering, Peoples' Friendship University of Russia
(RUDN University), 117198, Moscow, Russia.
Corresponding author: Mohammed Abdalla Elsharif Ibrahim,
e-mail: mohammedelsharif7@gmail.com.

Получена редакцией 07.03.2023; получена после рецензии 09.10.2023; принята к печати 10.03.2024.
Received by the editors 07.03.2023; received after the review 09.10.2023; accepted for printing 10.03.2024.